

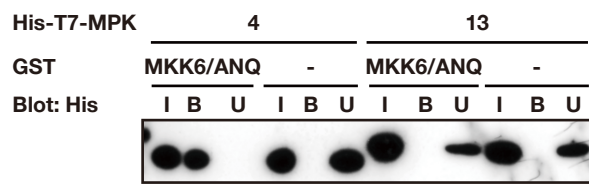
**Supplementary Fig. S1.** Expression of *MKK7* and *cyclin B1;1*.

Semi-quantitative RT-PCR was performed to determine the levels of transcripts of *MKK7* and *cyclin B1;1* in mature leaves, shoot apices and flowers using RNA isolated from plants that had been grown for 49 days in soil. The resultant cDNAs were amplified with primers specific for the two genes. We tested amplification by PCR with varying numbers of cycles, and the optimal number (as indicated in the Figure) for the most reliable results is shown for each gene. The gene for  $\alpha$ -tubulin was used as the control. Expression of *cyclin B1;1* has been reported in dividing cells (Ferreira et al., 1994; Colón-Carmona et al., 1999).

<References>

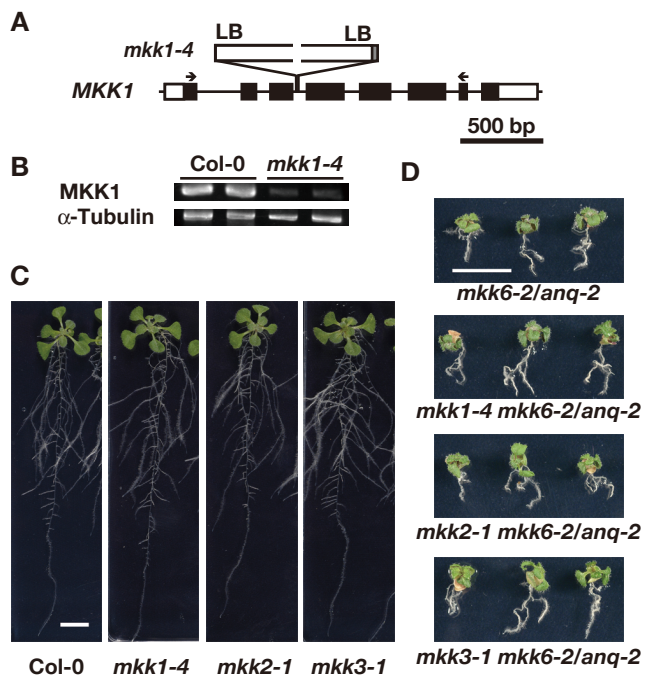
Colón-Carmona, A., You, R., Haimovitch-Gal, T. and Doerner, P. (1999) Technical advance: spatio-temporal analysis of mitotic activity with a labile cyclin-GUS fusion protein. Plant J. 20: 503-508.

Ferreira, P., Hemerly, A., de Almeida Engler, J., Bergounioux, C., Burssens, S., Van Montagu, M., Engler, G. and Inzé, D. (1994) Three discrete classes of *Arabidopsis* cyclins are expressed during different intervals of the cell cycle. Proc. Natl. Acad. Sci. USA 91: 11313-11317.



**Supplementary Fig. S2.** Coprecipitation of MPK4 and MKK6/ANQ.

Recombinant GST and GST-MKK6/ANQ were incubated separately with either His-T7-MPK4 (4) or MPK13 (13). Aliquots of both reactions were used as input fractions (I). Proteins were pulled down with glutathione-Sepharose 4B beads and each resultant precipitate (B) and supernatant (U) were visualized by immunoblotting with His tag-specific antibodies.



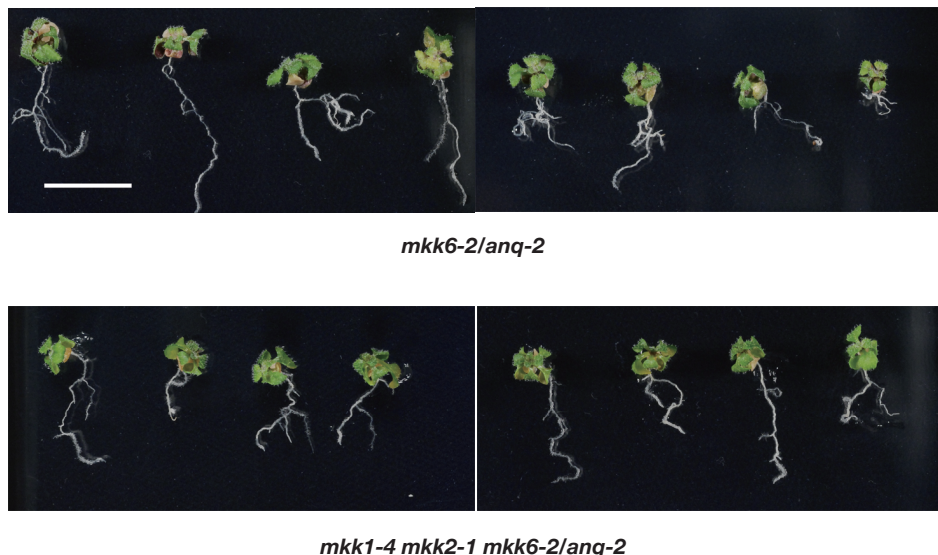
**Supplementary Fig. S3.** Double mutants that carried the *mkk6-2/anq-2* mutation plus a mutation in *MKK1*, *MKK2* or *MKK3*.

**(A)** Schematic representation of the *MKK1* gene. White boxes correspond to exons and black boxes indicate coding regions. The site of insertion of T-DNA in *mkk1-4* (SALK\_140054C) is indicated above the gene (not drawn to scale). LB indicates the left border of T-DNA and the open region in the T-DNA represents filler DNA.

**(B)** Analysis by RT-PCR of the *mkk1-4* mutant. Primer pairs depicted by arrows in **(A)** were used. RNA was extracted from entire above-ground parts of the plants that had been grown on plates. Two independent samples were used to ensure the validity of results.

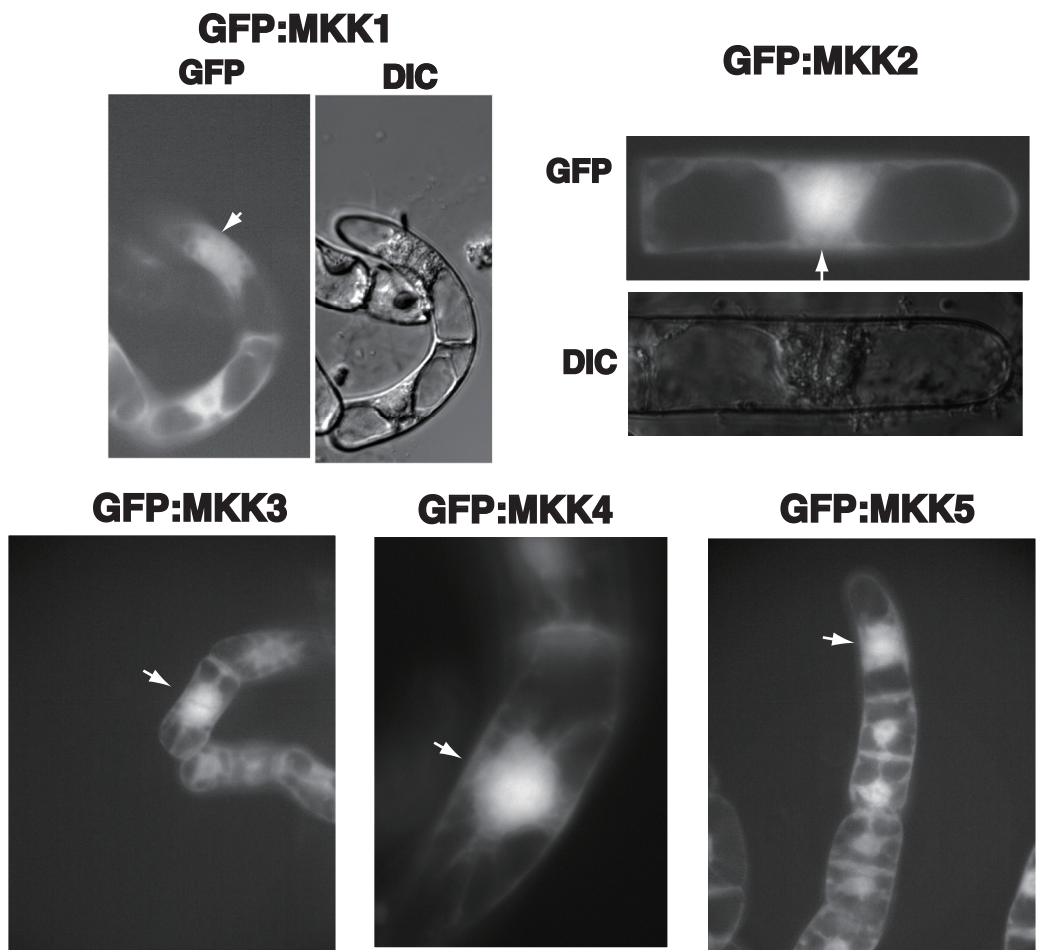
**(C)** Photographs of Col-0 and homozygous single-mutant plants after growth for 14 days on plates, at the same magnification. Both *mkk2-1* and *mkk3-1* have been reported to be null alleles (Teige et al., 2004; Takahashi et al., 2007). Bar, 1 cm.

**(D)** Photographs of *mkk6-2/anq-2* homozygous single-mutant plants and homozygous double-mutant plants after growth for 14 days on plates, at the same magnification. Bar, 1 cm.



**Supplementary Fig. 4.** Phenotype of the *mkk1-4 mkk2-1 mkk6-2/anq-2* triple mutant.

The *mkk6-2/anq-2* homozygous plants and *mkk1-4 mkk2-1 mkk6-2/anq-2* homozygous triple-mutant plants were grown for 14 days on plates. Plants are all shown at the same magnification. Bar, 1 cm.



**Supplementary Fig. 5.** Subcellular localization of GFP-MKKs.

The cDNAs encoding GFP-fused MKK1, MKK2, MKK3, MKK4 and MKK5 cDNAs were generated and expressed under the control of the 35S promoter of Cauliflower mosaic virus in BY-2 cells. Fluorescence due to GFP in cells at telophase (indicated by arrows) is shown. Nomarski images (DIC) are also shown in for GFP:MKK1 and GFP:MKK2. Arrows indicate cells in the stage of cytokinesis.

**Supplemental Table 1.** Primers used in this study.

Application	Sequence (5' – 3') (forward/reverse)	Description
RT-PCR of <i>anq-2</i> mutant	CTTGATTTCGAAATTACTGC/	Primer 2 in Fig. 1A
	CCAAAGATGATGCTCTTGCT	Primer 3 in Fig. 1A
RT-PCR of <i>anq-3</i> mutant	CAAGAATCCCCAATCTCTTCC/	Primer 1 in Fig. 1A
	TTATCTAAGGTAGTTAACAGG	Primer 4 in Fig. 1A
RT-PCR of <i>mkk1-4</i> mutant	TCCTCTTGAGCAATCCATCTC/ AATGATTGCGCTCTCATGATG	
RT-PCR of <i>MKK7</i>	CGTCAGGTGTCAAGGGATCT/ TCTGTCCCTGAGGAAGCAAC	
RT-PCR of <i>CycB1;1</i>	ATTGCAGACCATGCATAACAG/ CAAAGCGACTCATTAGACTTG	
qRT-PCR of $\alpha$ -Tubulin	GGACAAGCTGGGATCCAGG/ CGTCTCACCTTCAGCACC	Semiarti et al., 2001
qRT-PCR of <i>MKK1</i>	AGCAAAGGAGCTTCTGGAACAC/ TCCGAATCTCAAACATCTTACG	
qRT-PCR of <i>MKK2</i>	AGTTAAAGCCATCCCTGACTCCTAT/ AGCACTTGTCTAAAGATGGCAGAA	
qRT-PCR of <i>MKK3</i>	GAAAGGGAGAAAAGGCAGCAA/ CTTCACACAATGTCCGTATCTCTGT	
qRT-PCR of <i>MKK4</i>	CGTCGCCGTCTGATCTTAC/ CGAGAGAAACATCGCGTTGAG	

qRT-PCR of <i>MKK5</i>	CGTCCTTCGCTCTCAAAGTG/ TCTCACGGTATCTCGTGGTTTC	
qRT-PCR of <i>ANQ</i>	AGCTCTCCGTTCCAGCTCAA/ TCGCAGTCAGGAAGGAAGAGAT	
qRT-PCR of <i>MKK9</i>	AACAGTTAACGGCGACATGGA/ TCTCGCATCAACTGTCTTGAA	
qRT-PCR of $\beta$ -tubulin	ACCACTCCTAGCTTGGTGATCTG/ AGGTTCACTGCGAGCTCCTCA	Czechowski et. al. 2004

<References>

Czechowski, T., Bari, R.P., Stitt, M., Scheible, W.R. and Udvardi, M.K. (2004) Real-time RT-PCR profiling of over 1400 *Arabidopsis* transcription factors: unprecedented sensitivity reveals novel root- and shoot-specific genes. *Plant J.* 38: 366-379.

Semiarti, E., Ueno, Y., Tsukaya, H., Iwakawa, H., Machida, C. and Machida, Y. (2001) The *ASYMMETRIC LEAVES2* gene of *Arabidopsis thaliana* regulates formation of a symmetric lamina, establishment of venation and repression of meristem-related homeobox genes in leaves. *Development* 128: 1771–83.